



OPEN ACCESS

EDITED BY

Tomaso Fortibuoni,
Istituto Superiore per la Protezione e
la Ricerca Ambientale (ISPRA), Italy

REVIEWED BY

Milena Menna,
Istituto Nazionale di Oceanografia e di
Geofisica Sperimentale, Italy
Yoshikazu Sasai,
Japan Agency for Marine-Earth
Science and Technology (JAMSTEC),
Japan
Dagmar Hainbucher,
University of Hamburg, Germany

*CORRESPONDENCE

José C. Sánchez-Garrido
jcsanchez@uma.es

SPECIALTY SECTION

This article was submitted to
Marine Fisheries, Aquaculture and
Living Resources,
a section of the journal
Frontiers in Marine Science

RECEIVED 30 April 2022

ACCEPTED 06 July 2022

PUBLISHED 09 August 2022

CITATION

Sánchez-Garrido JC and Nadal I
(2022) The Alboran Sea circulation and
its biological response: A review.
Front. Mar. Sci. 9:933390.
doi: 10.3389/fmars.2022.933390

COPYRIGHT

© 2022 Sánchez-Garrido and Nadal.
This is an open-access article
distributed under the terms of the
[Creative Commons Attribution License
\(CC BY\)](https://creativecommons.org/licenses/by/4.0/). The use, distribution or
reproduction in other forums is
permitted, provided the original
author(s) and the copyright owner(s)
are credited and that the original
publication in this journal is cited, in
accordance with accepted academic
practice. No use, distribution or
reproduction is permitted which does
not comply with these terms.

The Alboran Sea circulation and its biological response: A review

José C. Sánchez-Garrido^{1,2*} and Irene Nadal^{1,2}

¹Physical Oceanography Group, Department of Applied Physics II, University of Málaga, Málaga, Spain, ²Instituto de Biotecnología y Desarrollo Azul (IBYDA), University of Málaga, Málaga, Spain

The oceanography of the Alboran Sea (AS) has been the subject of intensive research for decades. Chief among the reasons for this interest is the variety of physical processes taking place in the basin, spanning from coastal upwelling, dynamic of density fronts, internal waves, and strong meso- and submesoscale turbulence. Historical fieldwork and an increasing number of numerical studies in recent years have led to a more complete—although more dispersed—description and knowledge of process dynamics in the AS and their role in shaping primary productivity and regional fisheries resources. In this review, we summarize and put together old and new research to get an updated picture of the AS circulation and its variability at different time scales, with an emphasis on physical–biological interactions. As part of the review, we identify gaps in our understanding regarding the physical drivers for seasonal and for rapid transitions between the most recurrent one-gyre and two-gyre modes of circulation of the AS. We also point at possible research strategies based on end-to-end regional biophysical modeling to gain new insights into past and present physical control on fisheries resources and for assessing plausible climate change impacts on the AS ecosystem.

KEYWORDS

Alboran Sea, Strait of Gibraltar, nutrient fertilization, upwelling, tidal flow, small pelagic fisheries, ocean gyres, frontal jets

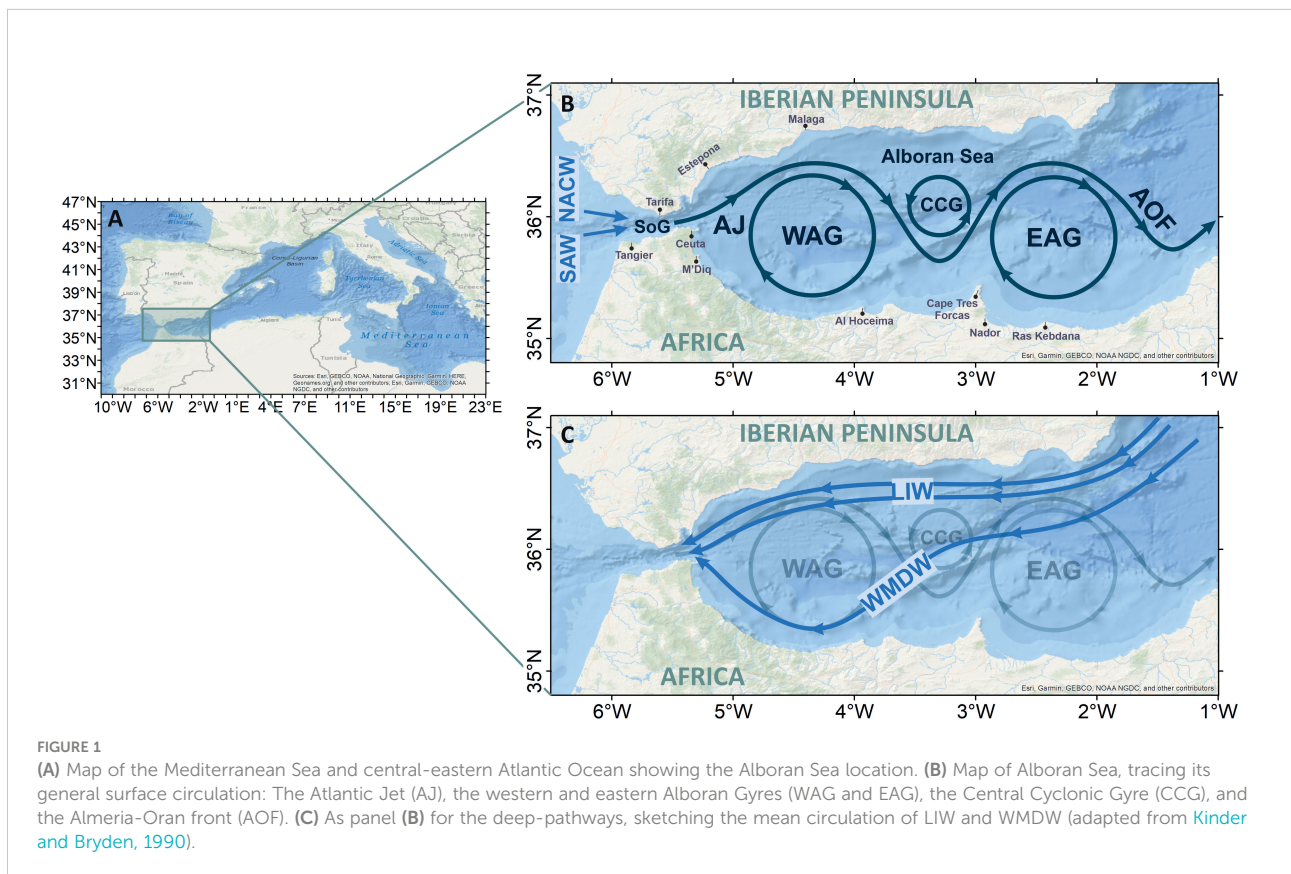
1 Geographical frame, mean circulation, and water masses

The Alboran Sea (AS) is the westernmost subbasin of the Mediterranean, extending from the Strait of Gibraltar (SoG) in the west to the imagery north-to-south line joining the locations of Almeria and Oran in the east (Figure 1). On this line typically lies the so-called Almeria-Oran front, which dynamically isolates the upper AS from the rest of the Mediterranean. The AS is some 150 km wide and 370 km long, and has a maximum depth of ~2,000 m. The continental shelf is narrow, typically less than 10 km wide and 100–150 m deep. The mean upper-layer circulation is characterized by a frontal jet of Atlantic Water (Atlantic jet, hereinafter AJ) surrounding two large-scale anticyclonic gyres, the so-called Western Alboran Gyre (WAG) and the Eastern Alboran Gyre (EAG) (Figure 1). A

smaller-scale cyclonic gyre typically lies in between. The AJ has a low salinity signal of ~36.6, extends over the surface 150–200 m, and features near-surface velocities of ~1 m/s or even more (Parrilla and Kinder, 1987). The AJ is ~30 km wide and forms a sharp density front with the denser ambient Modified Atlantic Water—up to 1 unit saltier than the incoming AW through the SoG; Cheney and Doblár (1982). Underneath, saltier and colder Levantine Intermediate Water (LIW; S = 38.5, T = 13.23°C) flows toward the SoG at 200–600 m depth. The LIW is broadly distributed in the basin, although it tends to accumulate on the Spanish slope deflected north by the Coriolis acceleration. The colder and denser Western Mediterranean Deep Water (WMDW; S = 38.48, T = 12.9°C) goes predominantly south from the NW Mediterranean, possibly driven by a major trough in the center of the basin (the AS Central Trough), heading towards the SoG banked against the African slope. Other intermediate and deep waters contribute to the Mediterranean outflow, the Tyrrhenian Dense Water and Winter Intermediate Water, although they represent a minor fraction with respect to the LIW and the WMDW (Naranjo et al., 2015).

The mean circulation determines overall biochemical patterns. The WAG and the EAG are characterized by horizontally convergent upper-layer circulation, downwelling, and a depressed pycnocline (interface between the Atlantic Water and the LIW)

situated at ~175 m depth (Viúdez and Tintoré, 1995; Vargas-Yañez et al., 2021). Conversely, the cyclonic region between the WAG and the EAG is associated with upwelling and exhibits an uplifted pycnocline (~50 m deep). This configuration is consistent with an ageostrophic Ekman circulation in the upper layer of the gyres induced by friction with the underlying LIW. The vertical excursion of the pycnocline and the nutrient-rich LIW (~9 μM of nitrate and ~0.4 μM of phosphate; Manca et al., 2004; Ramírez et al., 2021) shapes the vertical distribution of nutrients. Depressed nutricline is found within the WAG and EAG (~70–115 m; Moran and Estrada, 2001) and, accordingly, there is generally less primary production and lower concentration of surface chlorophyll (Ch) over the gyres (Figure 2A). Phytoplankton biomass is most abundant on the north coast of the AS and along the WAG and EAG peripheries. The first pattern is partly attributable to the baking of LIW against the north continental slope and the consequent shoaling of the pycno- and nutricline on this coastal margin. Regarding primary productivity, the largest values have been measured near the frontal regions between the WAG and the AJ, with average values of ~632 mg C m⁻² d⁻¹, while the minimum values correspond to the center of the WAG, with ~330 mg C m⁻² d⁻¹ (Moran and Estrada, 2001). Altogether, estimated annual primary productivity in the AS exceeds 100 g C m⁻² yr⁻¹, making it among the highest in the Mediterranean (Uitz et al., 2012).



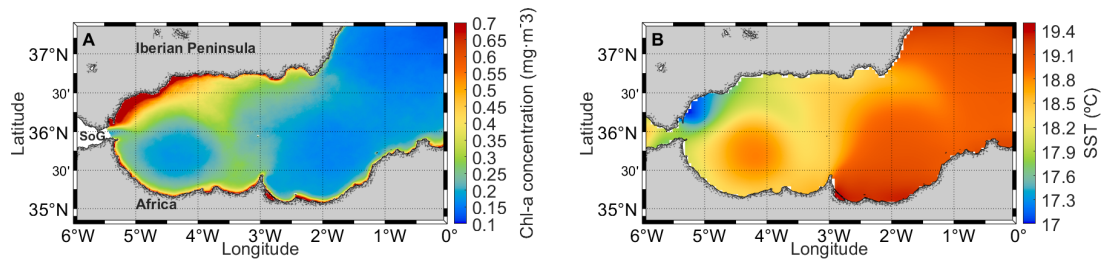


FIGURE 2

(A) Time-mean Chlorophyll-a concentration (mg/m^3) over the period 1997–2020 in the Alboran Sea, obtained from the CMEMS product OCEANCOLOUR_MED_CHL_L4_REP_OBSERVATIONS_009_078. (B) Time-mean Sea Surface Temperature (SST) over the period 1981–2021 in the Alboran Sea, obtained from the product SST_MED_SST_L4_REP_OBSERVATIONS_010_021.

2 Origin and maintenance of the mean circulation

Laboratory experiments and numerical simulations indicate that the WAG and EAG originate from loop currents that form off Ceuta and Cape Tres Forcas (Whitehead and Miller, 1979; Oguz et al., 2014). Such currents are fed by the AJ, which in the absence of the WAG and the associated high-pressure anomaly tends to veer south because of the Coriolis acceleration to later follow the African coast. The formation of the loop currents and the establishment of the mean circulation have been attributed to the abrupt change of orientation of the coastline at Ceuta and Cape Tres Forcas (Bormans and Garrett, 1989; see locations in Figure 1). In these locations, the radius of curvature of the coastline is shorter than the inertial radius, $r = U/f$ (U is the current velocity and f the Coriolis frequency), which corresponds to the theoretical radius of curvature of the trajectory of the jet in the absence of external pressure gradients. Thus, after surpassing Ceuta and Cape Tres Forcas, the AJ separates momentarily from the coast to impinge it again at some location downstream (east). The incident angle of the jet is large enough to generate a loop coastal current (or “separation bubble”) that recirculates anticyclonically. After their genesis, these small-scale currents grow fed by the AJ until reaching basin-wide dimensions, turning into the WAG and EAG themselves. The whole process lasts for 90–120 days (e.g., Oguz et al., 2014), after which both the WAG and EAG become essentially geostrophic balanced.

Once formed, a question that has attracted much attention is how the gyres maintain their heat, salt, and momentum budgets against mixing and dissipation. This question has concerned especially the WAG, probably because it is a more recurrent and long-standing feature than the EAG (Renault et al., 2012). Bryden and Stommel (1982) argued that the upward flow of WMDW over the African slope toward the SoG is a source of anticyclonic vorticity that keeps the WAG spinning against friction. The uplift of WMDW would be in turn a consequence of the outflow of LIW through the SoG, whose high velocity over the sill (~ 1 m/s) creates a

dynamic pressure reduction that makes possible the drainage of deep waters. The term “Bernoulli aspiration” was coined to describe the process (Kinder and Bryden, 1990).

The Atlantic inflow has also been suggested to play some role in the maintenance of the WAG. Viúdez and Haney (1997) reported the existence of a permanent subsurface salinity minimum at the core of the WAG, from which it was postulated that some flow of Atlantic Water must enter the WAG ageostrophically (i.e., crossing isobars) directly from the Strait, perhaps mediated by tidal flows. The renewal of Atlantic Water in the WAG would help maintain its horizontal density gradient with ambient waters and thereby its geostrophic motion *via* thermal wind balance.

Brett et al. (2020) have recently shown from the numerical simulation of a quasi-steady WAG that its low salinity and warm temperature signals, as well as its negative vorticity budget, are not held constant but are gradually eroded by advection of ambient Modified Atlantic Water into the gyre. The salinity minimum at the center of the WAG identified by Viúdez and Haney (1997) would originate from its early formation in its loop-current stage to later decay over time. However, the dissipation of the WAG occurred so slowly that changes in the properties of the WAG were practically inappreciable over the 5-month numerical run.

3 Mesoscale and seasonal variability

The notion of a quasi-steady WAG in the previous is somewhat idealized because abrupt changes of the WAG, including its collapse (i.e., a rapid weakening) or its migration toward the eastern AS have been observed (Perkins et al., 1990; Viúdez and Haney, 1997; Flexas et al., 2006). In such situations, the AJ becomes a coastal jet that follows the African coast and the circulation in the western AS becomes predominantly cyclonic (Peliz et al., 2013). Satellite imagery shows that the AJ can maintain its coastal-jet configuration for up to two months until a perceptible WAG develops (Vargas-Yáñez et al., 2002).

Collapse and migration events of the WAG occur mainly during the fall and winter and largely determine the seasonality of the AS surface circulation (Vargas-Yáñez et al., 2002; Renault et al., 2012). Analysis of a 20-year simulation by Peliz et al. (2013) shows that the migration of the WAG and its subsequent interaction with the EAG can cause dramatic changes in the latter—e.g., one possible scenario is that both gyres merge and drift east by the Algerian Current—, suggesting that the seasonality of the EAG can be in part inherited from the WAG. This conclusion is supported by the fact that the two gyres show qualitatively similar seasonal variability, both being weaker during winter (the EAG being more elusive) and more frequent and with the largest sizes in summer (Figure 3).

The origin of the seasonal variability of the AS circulation and the drivers for the collapse and migrations of the WAG have been addressed in several investigations, most of them pointing at a possible of the inflow through the SoG (Vargas-Yáñez et al., 2002; Vélez-Belchí et al., 2005). Vargas-Yáñez et al. (2002) reported a migration episode of the WAG preceded by a significant drop of the inflow caused by meteorological forcing (storm surge flows). Meteorologically driven flows in the SoG largely account for changes in seal-level pressure over the Mediterranean (Candela et al., 1989; García-Lafuente et al., 2002), and can be large enough to halt the inflow (~ 0.8 Sv)—or double its magnitude—for few days (García-Lafuente and Delgado, 2004). It was speculated that the migration of the WAG was triggered by the shortening of the inertial radius of the AJ, which caused its veering toward the African coast. The stronger

subinertial variability of the inflow in autumn and winter associated with the passage of synoptic atmospheric systems over the Mediterranean would be consistent with the more frequent migrations of the WAG during this time of the year. Other authors have suggested that the variability of the inflow caused by the freshwater seasonal cycle of the Mediterranean can also determine the seasonality of the WAG (Renault et al., 2012). This hypothesis seems questionable because the inflow has a minor seasonal amplitude of ~ 0.03 – 0.04 Sv (Soto-Navarro et al., 2010), one order of magnitude smaller than subinertial fluctuations. Moreover, the AJ and WAG can adjust geotropically (quasi-steadily) to the long-scale seasonal signal of the inflow.

High-resolution numerical simulations have offered insights into the circumstances preceding the migration of the WAG. Sánchez-Garrido et al. (2013) showed that the blocking of small-scale cyclonic eddies (~ 10 km) traveling around the WAG periphery, trapped between the AJ and the north coast of the AS, can trigger the south deflection of the AJ and ultimately force the WAG to migrate. These eddies originated from the separation of the northern lateral boundary layer of the SoG; eddies with anticyclonic vorticity were shed from the south boundary, leading to a Kármán vortex street. Positive and negative vorticity fluxes toward the AS, as well as the size of the generated eddies, increased with strong time dependence of the flow. The most dramatic events of eddy generation occurred when the AJ entered the AS forming a vortex dipole—mushroom-like current—after recovering from a weakening period of a few days due to adverse (westward) meteorologically-driven flows (Figure 4). This type of event is

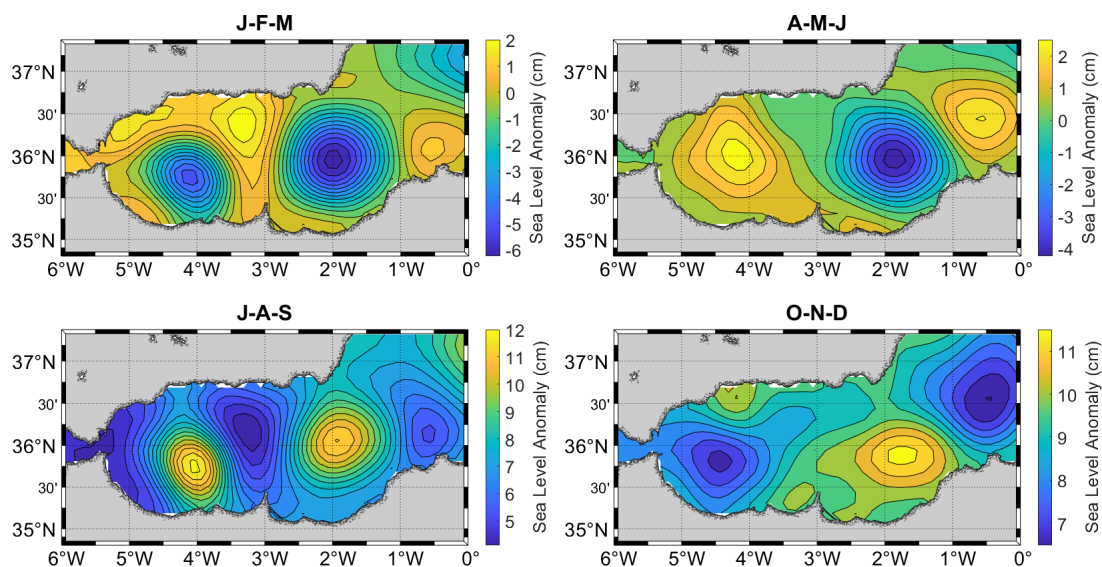


FIGURE 3

Seasonal climatology of Sea Level Anomaly (SLA) in the Alboran Sea (period 1993–2021). Isolines are shown every 0.5 cm. J-F-M: January–February–March, A-M-J: April–May–June, J-A-S: July–August–September, O-N-D: October–November–December. CMEMS product: SEALEVEL_EUR_PHY_L4_MY_008_068.

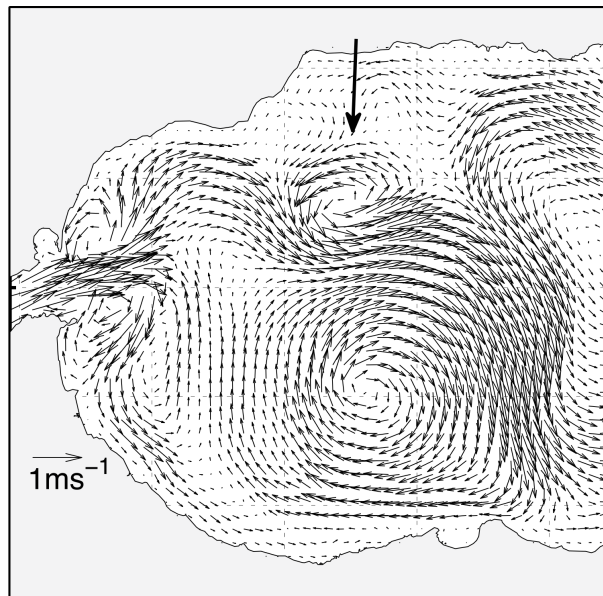


FIGURE 4

Snapshot of the surface velocity field in western Alboran from numerical simulations. The arrow indicates a cyclonic mesoscale eddy surrounding the WAG. The AJ enters the AS as a mushroom-like (ageostrophic) current. This current structure is associated to intensified inflow through the SoG by incoming meteorologically-driven flows (adapted from Sánchez Garrido et al., 2015; see this paper for other synoptic situations).

more frequent in winter, associated with the greater variability of sea-level pressure over the Mediterranean during this season.

The time variability of the flow through the SoG was unable to explain, however, most of the collapses/migrations of the WAG identified in the numerical run of Peliz et al. (2013). The most recurrent double-gyre structure (up to 48% of the time) tended to occur during periods of large internal Rossby Radius (stronger stratification) and mild winds, suggesting a possible role of eddy dynamics and intrinsic variability of the basin, rather than conditions externally forced by conditions in the SoG, in determining stability periods and alternance between one-gyre and two-gyre circulation types. Peliz et al. (2013) also found that cyclonic mesoscale eddies in the AS (of ~13 km) were most common in winter, outnumbering by far anticyclonic eddies. This links with the result of Brett et al. (2020), who noted a slow decay of the WAG by advection of cyclonic vorticity into the gyre. The decay of the WAG in winter could be hence related to the dominance of cyclonic eddies (and the consequent cyclonic vorticity anomaly) in the basin.

4 Submesoscale variability

Both meso- and submesoscale (<10 km) eddies have been observed traveling along the WAG periphery. These features were probably first reported by La Violette (1984), who noted cold-water rings around the WAG in high-resolution satellite imagery. García-

Lafuente and Delgado (2004) investigated the meandering trajectory of a drifter around the WAG accidentally released at the eastern part of the SoG. The wavy path of the drifter was attributed to its trapping by a submesoscale eddy with an origin at the SoG. Both La Violette and Lacombe (1988) and García-Lafuente and Delgado (2004) point to tidal pulses of vorticity generated in the Strait, later carried by the AJ, as the likely origin of these eddies. These findings concur with the numerical results of Sánchez-Garrido et al. (2013), although the most obvious eddies found by these authors, were associated with subtidal time dependence of the flow (meteorologically-driven flows). The non-recurrent presence of these eddies in satellite images suggests that they are not necessarily tidally driven. Another possibility is that these features are too small to be detected regularly by remote sensing devices. In addition to small-scale eddies arising from the SoG, significant submesoscale activity occurs in the vicinity of the AJ associated with its nonlinear frontal dynamics (see *Frontal dynamics*).

5 Nutrient enrichment mechanisms

5.1 Mixing in the SoG

5.1.1 Mixing in the steady exchange

The Atlantic Water entering through the SoG is composed of surface Atlantic Water and colder and nutrient-richer North

Atlantic Central Water. This inflow is enriched through the Strait because of vertical mixing with the underlying Mediterranean Water. Two-layer hydraulics provides guidance as to where and how vertical mixing occurs through the Strait (Armi, 1986; Pratt and Whitehead, 2008). A useful dimensionless number is the internal composite Froude number

$$G^2 = F_1^2 + F_2^2$$

where $F_1^2 = u_1^2/g'h_1$ and $F_2^2 = u_2^2/g'h_2$; here, u_i and h_i denote velocity and thickness of the surface ($i=1$) and bottom layers ($i=2$), and $g' = 2g(\rho_2 - \rho_1) / (\rho_2 + \rho_1)$ is the reduced gravity. The hydraulic state of the flow is determined by the value of G^2 . The flow is classified as critical, subcritical, or supercritical according to $G^2 = 1$, $G^2 < 1$, or $G^2 > 1$, respectively. The flow criticality can be interpreted in terms of the direction that information can travel through the flow by long interfacial waves. Critical flow ($G^2 = 1$) implies that one of the two interfacial waves supported by the flow is stationary (i.e., it has null phase velocity). Subcritical flow ($G^2 < 1$), typically occurring in relatively stagnant regions, implies that the two waves travel in opposite directions. Similarly, in supercritical regions ($G^2 > 1$) both waves propagate in the same direction. An important consequence is that the flow can become unstable (with respect to long waves) only in critical or subcritical regions—mathematically, the phase speed of the interfacial disturbances becomes complex conjugates. Therefore, strong mixing due to instabilities is expected to occur where the flow turns supercritical. Other recognized locations where intense mixing occurs are across hydraulic jumps, regions of the flow matching supercritical-to-subcritical conditions.

In the SoG, there is one critical section over the Camarinal Sill and a second critical section at the Tarifa Narrows (Armi and Farmer, 1988; Kinder and Bryden, 1990; García-Lafuente et al., 2000; Figure 5A), although the presence of this latter section has been suggested to be non-permanent (Garrett et al., 1990). The flow at these two sections is said to be hydraulically controlled. Immediately west and east of these two control sections are two supercritical regions, each followed by hydraulic jumps matching subcritical conditions in the connecting seas—the Gulf of Cadiz and the AS. Hence, enhanced mixing occurs immediately west of Camarinal Sill in the so-called Tangier basin, and east of Tarifa Narrows (Figure 5A). In these locations of the Strait, mixing creates an obvious intermediate mixing layer that has motivated the consideration of a three-layer model to better represent the structure of the flow (Figure 5B; Bray et al., 1995; Sannino et al., 2009). Estimates of the mixing layer thickness (ΔZ) (sketched in Figure 6A) in the hypothetical steady flow sketched in Figure 5B vary from 15 m in the Camarinal Sill to 50–80 m in the eastern part of the SoG and in the Tangier basin (Naranjo et al., 2014; Figure 6B).

5.1.2 Tidal flows and residual

The steady picture of the flow through the SoG is modified by time-dependent flows, particularly tides. Tidal flows reach peak

values of up to 6 Sv, with ~3 Sv associated with the M_2 tidal constituent alone (García-Lafuente et al., 2000). The first tidal implication is the input of mechanical energy available for mixing. A second implication is the periodic reversal of both the Atlantic and the Mediterranean layers over the Camarinal Sill, so that for some time during the tidal cycle the two-way structure of the flow is temporarily lost, with both layers pointing in the same direction. This has important hydraulic consequences as well as for the dynamics of the interface mixing layer.

During the flood tide (westward tidal flow), the Mediterranean outflow current is tidally intensified, leading to faster-growing instability and enhanced mixing within the supercritical region west of Camarinal Sill. Here, Wesson and Gregg (1994) reported peak values of energy dissipation rates of up to $10^{-2} \text{ W kg}^{-1}$ (hundreds of times larger than in the open ocean) and the presence of Kelvin–Helmholtz billows. Enhanced energy dissipation and mixing also occur across the now larger hydraulic jump west of Camarinal Sill (Sánchez-Garrido et al., 2011). As a result, an enlarged pool of mixed water is created in the Tangier basin at the end of the flood tide.

During the ebb tide (eastward tidal flow), the Mediterranean layer reverses and the Atlantic flow strengthens. The Atlantic current entrains part of the pool of mixed water that had formed in the Tangier basin during the previous few hours (Figure 5C). García-Lafuente et al. (2013) estimated that as much as 30% of the pool ultimately contributes to the inflow. One effect of the tides is therefore to add nutrient-rich mixing water into the inflow. This is reflected in the widening of the interface mixing layer at the eastern part of the SoG with respect to a non-tidal situation (Figure 6B, C).

Tides also raise the mixing layer in the eastern part of the SoG. This second effect can be understood from the upstream influence exerted by a sill-controlled flow (Pratt and Whitehead, 2008). For sill-controlled flows resembling a flow spilling down a dam, such influence is regulated by a nonlinear weir formula that links the flow rate with the height of the fluid at the dam, so that variation in one of the two magnitudes perturbs the other. In the SoG, the interface east of Camarinal Sill moves up and down in response to changes in the tidal flow rate. The net (mean) effect of the back-and-forth movement of the tides leaves the interface—taken at the mid depth of the mixing layer—shallower than in the unperturbed non-tidal flow (Figures 6D, E), further favoring primary production.

A third tidally-driven process is the radiation of large-amplitude internal waves (~100 m amplitude) from the Camarinal Sill to the AS (Figure 5C; Sánchez-Garrido et al., 2008; Sánchez-Garrido et al., 2011). These waves evolve from the internal hydraulic jump formed in the Camarinal Sill, which propagates eastward when hydraulic control is lost over the sill ($G^2 < 1$) as the Mediterranean current weakens. The nonlinear evolution of the hydraulic jump leads to a series of internal solitary waves. Although these waves can drive dramatic vertical oscillations of 100 m in only 20–30 min (Vlasenko et al., 2000), their role in the overall water mixing occurring in the SoG seems to be secondary. Solitary waves propagate for hundreds of kilometers with minor energy (amplitude) loss (Jackson and

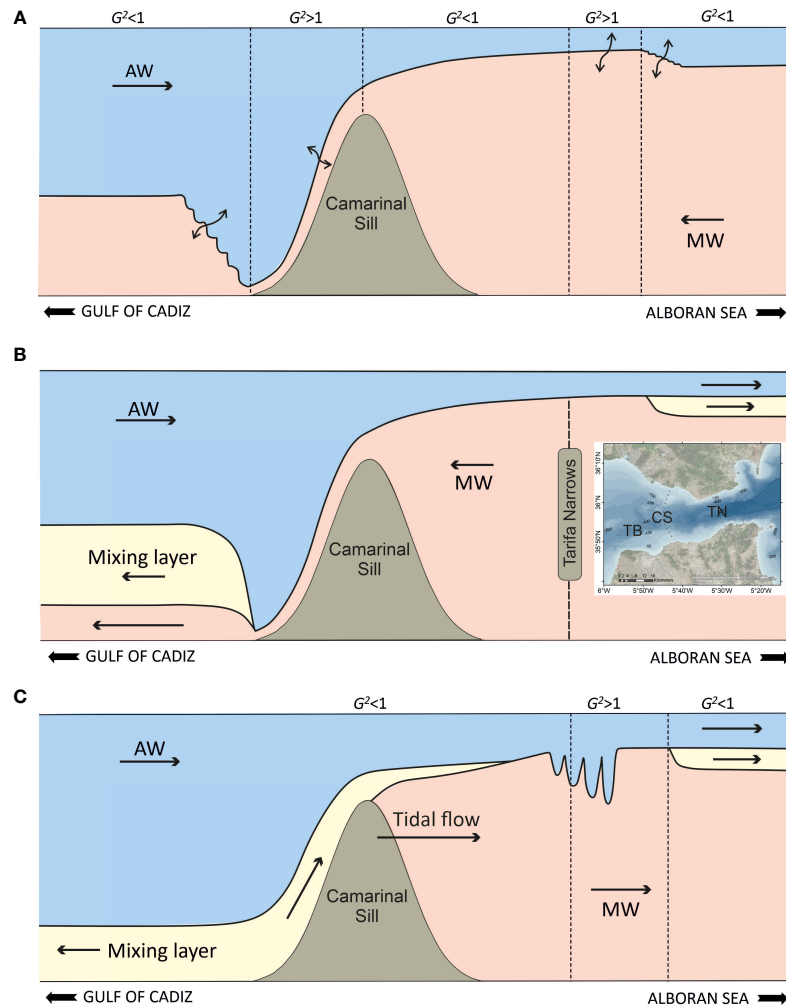


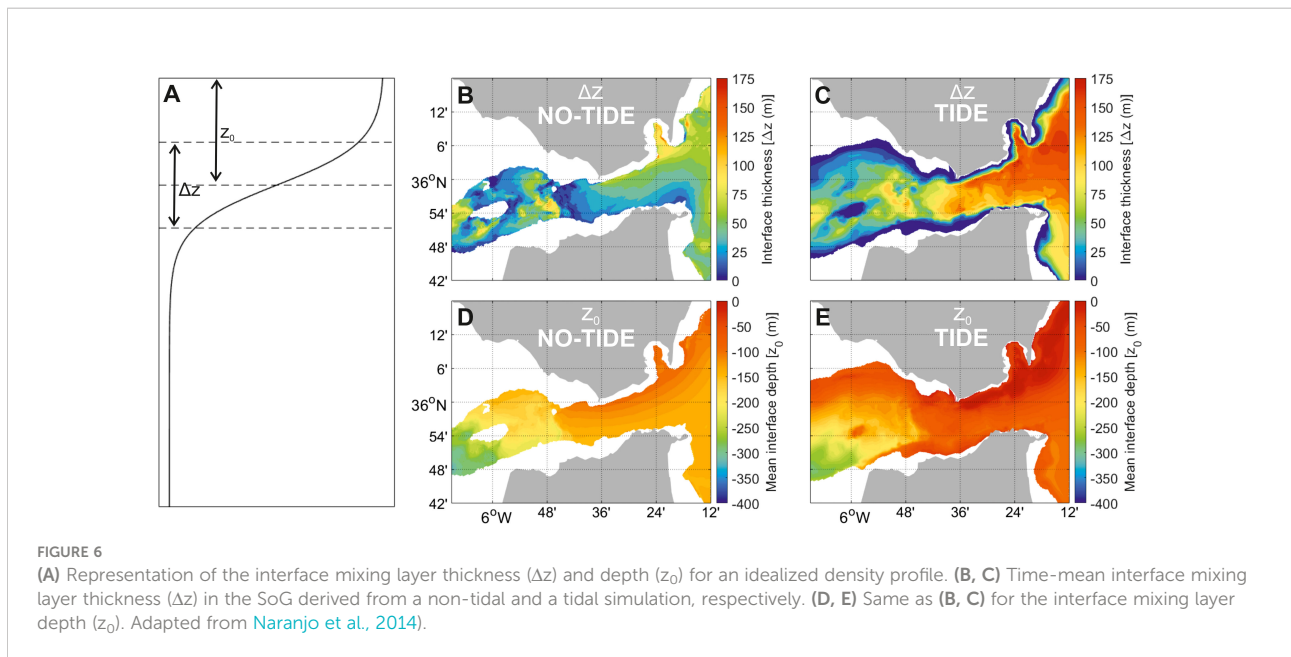
FIGURE 5
 Sketches of the flow through the SoG. **(A)** The steady two-layer maximal exchange with internal hydraulic control at the Camarinal Sill and at the Tarifa Narrows. Double arrows indicate regions of enhanced mixing. The wiggling interface represents internal hydraulic jumps. **(B)** Three-layer representation of the steady flow through the SoG. Vigorous mixing has created an intermediate mixing layer that widens towards both ends of the strait (particularly west of the Camarinal Sill where mixing is strongest). The inset shows the location of the Camarinal Sill (CS) and the Tarifa Narrows (TN) within the Strait. **(C)** Snapshot of the tidally-forced three-layer exchange. Tidal flow points towards the AS; hydraulic control has been lost over the sill and the hydraulic jump can now propagate eastward, breaking up into a series of solitary waves. The Mediterranean layer over the sill has been reverted by the tidal flow, allowing for the intrusion of mixing water from the Tangier Basin (TB in the inset; west Camarinal Sill) into the AS.

Apel, 2004). The clear signature of solitary waves propagating across the AS in remote sensing images (Alpers et al., 2008) suggests that only a small fraction of their initial energy is dissipated within the SoG, probably because of partial wave breaking at the Strait’s lateral boundaries (Vlasenko et al., 2009).

5.1.3 A note on the nutrient-enriched inflow and phytoplankton response

The described tidal processes lead to a nutrient-enriched inflow exposed to light at the eastern part of the SoG. Reported average nutrient concentrations of the inflow are ~3.0 μM for

nitrate and ~0.25 μM for phosphate (Gómez et al., 2000; Huertas et al., 2012), much larger than typical phytoplankton semi-saturation constants ($K_{NO_3} = 0.5 \mu M$, $K_{PO_4} = 0.05 \mu M$; Eppley et al., 1969; Davies and Sleep, 1989). Despite the fertile inflow, phytoplankton biomass is relatively scarce within the Strait itself (Echevarría et al., 2002; Ramírez et al., 2014), a fact that can be understood from the short residence time of phytoplankton within the channel (Macías et al., 2009), estimated at ~10 h ($L/U = 10$ h; with $L = 36$ km, the distance from Tarifa to the eastern part of the Strait, and $U = 1$ m/s is a typical flow velocity). Considering a typical phytoplankton



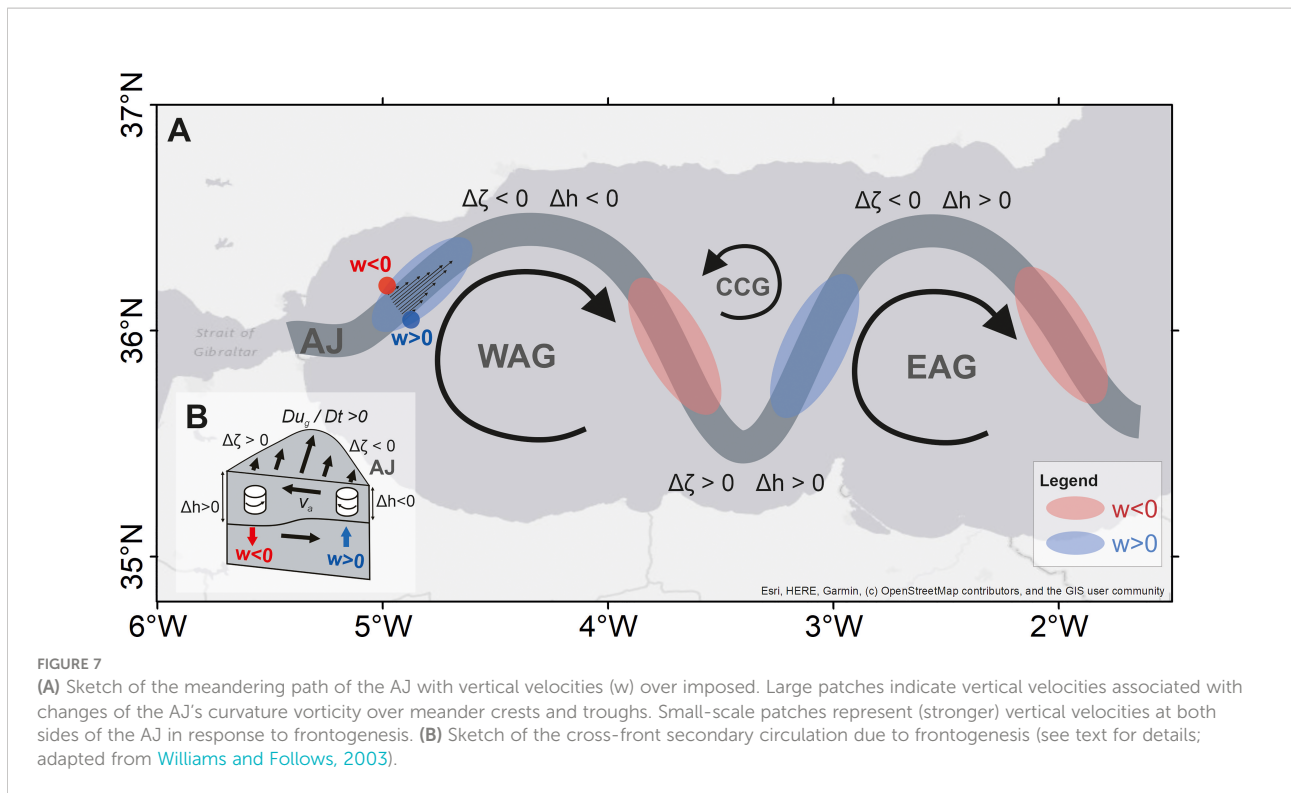
doubling time of 1 day, a time span of 10 h is indeed too short for phytoplankton to grow significantly. The bulk of the nutrients carried by the AJ are consumed downstream in NW Alboran. Sánchez Garrido et al. (2015) estimated that the nutrient supply by tidal mixing in the SoG represents as much as ~37% of the total biomass and primary productivity in western Alboran.

5.2 Frontal dynamics

The ageostrophic frontal dynamics of the AJ is another source of fertilization of the AS surface waters. In a general context, the permanent density fronts of the AS make this sea an ideal setting for investigating the dynamics of density fronts, characterized by large vertical velocities (w) and enhanced primary productivity. Tintoré et al. (1990) and Gomis et al. (2001) estimated vertical velocities of the order of $\sim 15 \text{ m d}^{-1}$ in western Alboran based on the omega equation (Holton, 2004). These calculations hence rely on quasi-geostrophic theory and the assumption of slight departures from geostrophic balance, as quantified by a small Rossby number, $Ro = U/fL \ll 1$ (U is the downstream velocity component, L is the transversal length scale of the AJ, and f the Coriolis frequency). The pattern of vertical velocity was such that upward and downward motions occurred upstream of meander crests and troughs, respectively (Figure 7A). A similar structure has been found in the Gulf Stream and in atmospheric jet streams (Newton, 1978; McWilliams et al., 2019 and references therein). The pattern is consistent with changes in the relative vorticity of the jet $\zeta = \partial v / \partial x - \partial u / \partial y$ being controlled by curvature vorticity over crests and

troughs, so that the jet is vertically stretched and squeezed over these regions to conserve potential vorticity ($\zeta + f)/h$ (here h is the vertical thickness of the jet).

The biological impact of the AJ frontal dynamics was investigated by Oguz et al. (2014) by means of process-oriented biophysical modeling. Large vertical velocities in the AJ ($\sim 30 \text{ m d}^{-1}$) gave rise to enhanced primary productivity and patches of phytoplankton biomass, which were then advected along the jet and stirred and dispersed within the basin by mesoscale eddies. Although the overall spatial pattern of the simulated w was consistent with previous results, finer-scale patchiness suggested an important role of submesoscale processes in driving vertical motions along the AJ. A nonlinear dynamic of the AJ beyond the formal applicability of quasi-geostrophic theory is indeed expected provided the finite Rossby number involved, $Ro \sim 1$ (Sánchez-Garrido et al., 2013; Oguz et al., 2014). In such cases, vertical velocities are often due to frontogenesis; namely, rapid intensifications of cross-front density gradients that result in temporary breakdowns of geostrophic balance—frontogenesis itself can be caused by large-scale geostrophic flow tending to align lateral density gradients. Capó et al. (2021) have recently shown that frontogenesis is indeed a recurrent feature of the AS fronts. Frontogenesis prompts a cross-front vertical circulation cell with upward and downward motions at either side of the front. The origin and characteristics of this secondary ageostrophic current have been amply described in the literature of frontogenesis dynamics (Spall, 1995; McWilliams, 2021) and will now be summarized shortly. For an eastward propagating jet, the downstream acceleration of the flow in response to a rapid increase in the cross-front pressure gradient is balanced by the Coriolis acceleration. This statement follows from the quasi-



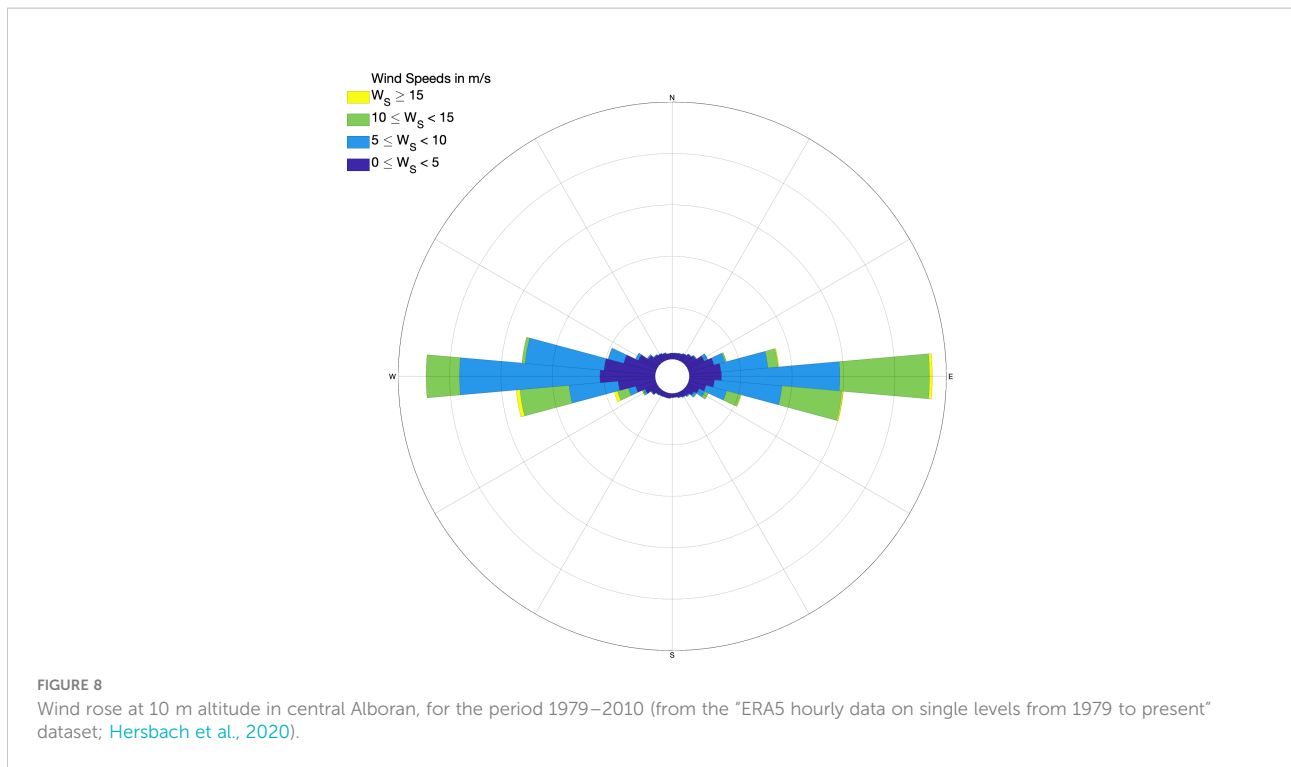
geostrophic horizontal momentum equation, $Du_g/Dt = fv_a$ (subscripts “g” and “a” denote the geostrophic and ageostrophic contributions of the velocity field). For the prevailing eastward AJ, this balance implies a northward surface current from its anticyclonic side (south) to its cyclonic side (north) in response to frontogenesis. Stronger downstream flow also leads to enhanced anticyclonic (shear) vorticity in the anticyclonic side of the AJ and enhanced cyclonic (shear) vorticity in its cyclonic side, requiring upwelling in the first and downwelling in the latter for potential vorticity to be conserved (Figure 7B). Nondivergence of the ageostrophic circulation demands that a countercurrent flows underneath the jet. The direction of the ageostrophic circulation cell would be inverted in the case of a sudden drop in the horizontal density gradient (i.e., frontolysis).

Evidence of submesoscale frontal dynamics in the AS is scarce given the observational challenges derived from the short spatial and temporal scales involved. The most comprehensive process-oriented set of observations was probably collected by Pascual et al. (2017) and Ruiz et al. (2019) in eastern Alboran, using various instrumentation, including a set of underwater gliders and surface drifters. The footprint of submesoscale dynamics in the Almeria-Oran front was revealed by the subduction of Chl up to 60 m below the deep Chl maximum. Although observational evidence is still required, submesoscale vertical velocities are expected to be stronger around the edges of the WAG, given the sharper density fronts of this region (Oguz et al., 2014; García-Jove et al., 2022). The role of submesoscale dynamics in overall phytoplankton production and

export in the ocean, and in the AS in particular, is currently a subject of active research (Troupin et al., 2019; Esposito et al., 2021; Zarokanellos et al., 2022).

5.3 Coastal upwelling

Winds are mainly zonal in the AS (Figure 8). Easterlies and westerlies blow with the same strength and are similarly likely except for slight seasonal variations. The strongest winds in either direction—east or west—occur during the winter, whereas the mildest winds are found during the summer. In the summer, easterlies are also somewhat more frequent than westerlies. The overall zonal orientation of the AS shoreline makes it suitable for wind-driven coastal upwelling to occur either on the north or the south coast of the basin. Offshore Ekman transport and upwelling is driven by westerlies on the north and easterlies on the south. Despite the bimodality and symmetry of the wind regime, wind upwelling episodes turn out to be more recurrent and stronger along the Spanish coast. This north-south asymmetry is well noticed in satellite imagery of SST and ocean color, which generally shows cooler and biomass-richer waters in the north of Alboran in response to wind forcing. The shallower pycnocline and nutricline in north Alboran, resulting from the banking of LIW against the Spanish slope, are the candidate background conditions explaining the more vigorous ocean response to wind forcing in this part of the basin.



Coastal upwelling not caused by wind has also been documented in NW Alboran off Estepona. Recurrent high Chl concentration and cool SST in satellite images suggest the presence of a quasi-permanent upwelling in this region (Figure 2A, B), although part of this signal is probably accounted for advection of mixing water from the SoG. [Sarhan et al. \(2000\)](#) reported upwelling off Estepona associated with offshore excursions of the AJ. The AJ was observed to move offshore over a time scale of 1 week, leading to near-shore upward velocities of $\sim 10 \text{ m d}^{-1}$ from the mass conservation principle. Such vertical velocity implies a more moderate, but also more recurrent, upwelling than that caused by strong westerly winds. The proposed upwelling mechanism is persistent insofar as the AJ flows close to the coast, which in turn requires the presence of a well-developed WAG.

6 Physical–biological interactions during early life stages

The AS supports regionally important fisheries of anchovy and sardine ([Giráldez, 2021](#)). Nutrient enrichment and the consequent planktonic production (food supply) are the primary processes sustaining these fish populations. Enrichment is the main environmental characteristic of the triad proposed by Bakun ([Bakun, 1996](#); [Agostini and Bakun, 2002](#)) for suitable spawning and nursery habitats; the other two propitious features are concentration and retention. Concentration, i.e., flow convergence, leads to the patchiness of aggregate plankton biomass and fish larvae, guaranteeing good feeding conditions for

the latter. Retention characteristics help maintain fish early life stages—eggs and larvae—within the favorable nursery habitat.

Some coastal regions of the AS satisfy the conditions of the so-called “Bakun triad.” Overall, the north coast is a more appropriate habitat than the south coast because of its higher food availability. The Estepona area and the Bay of Malaga are the main spawning and nursery grounds for anchovy and sardine. [García et al. \(2021\)](#) noted distinct environmental characteristics possibly limiting recruitment in the two areas. The Estepona region is abundant in food, but also openly exposed to the dispersal of early life stages by the AJ and by meso- and submesoscale eddies surrounding the WAG (Figure 4). The Bay of Malaga, relatively sheltered from the AJ because of the local shoreline and its wider continental shelf ($\sim 20 \text{ km}$), is less biologically productive than the Estepona region but has better retention characteristics. Leaving aside local habitat differentiations, the degree of recruitment in north Alboran as a whole depends on food supply, onshore retention of early life stages, and near-surface seawater temperature (*via* constrains of reproductive phenology and bioenergetics). These environmental conditions are largely mediated by the strength and direction of the AJ as well as by wind forcing. Inter-annual variability and trends of these conditions are assumed to play a central role in shaping ups and downs and long-term decline of anchovy and sardine recruitment (and landings) in north AS (Figure 9).

The dependence of recruitment on environmental conditions is difficult to be established because the latter also affects fish behavior. For example, the spawning strategy of sardines in north Alboran seems to depend on wind ([García et al., 2021](#)). Sardine prefers to spawn during calm wind periods

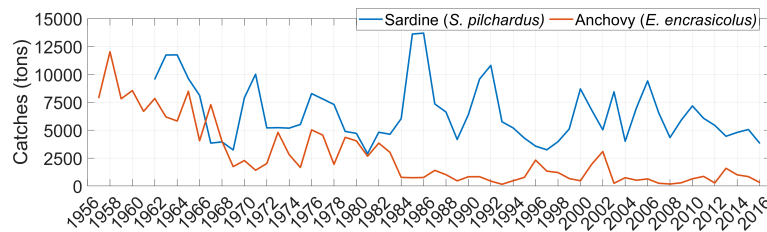


FIGURE 9

Time series of sardine (blue) and anchovy (red) landings in north Alboran. Data were obtained from the official statistics of the General Fisheries Secretariat (SGPM), Fisheries Regulatory and Market Fund (FROM), and the Spanish Institute of Oceanography (IEO).

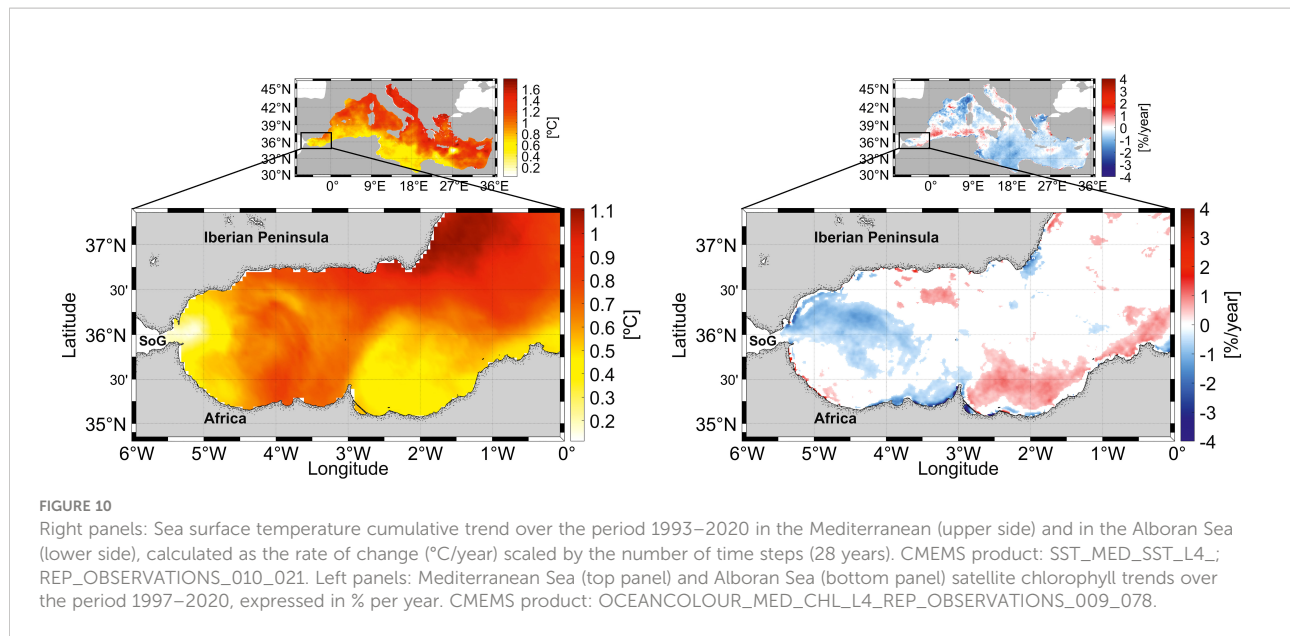
soon after strong upwelling events by westerlies have fertilized the north coast of the AS, in an attempt to maximize both larval growth and retention (García, 2006). Overall, repeated upwelling events during the spawning season (autumn-to-winter) seem to be beneficial, provided that yearly westerly winds and Chl appear positively correlated with sardine landings in north AS (Vargas-Yáñez et al., 2020). Anchovy recruitment seems to be less dependent on the wind, perhaps because this species spawns during summer, the season of the year in which winds are mildest and do not account for much of the environmental variability. The anchovy population seems to be linked to the direction and strength of the AJ, with enhanced AJ and WAG negatively impacting the anchovy recruitment in north Alboran (Ruiz et al., 2013). The positive effect of added food supply in this region associated with a stronger AJ-WAG system (Navarro et al., 2011) would thus be overcome by exacerbated dispersion of early life stages by the same flow pattern.

Fisheries studies in south Alboran are scarcer. Annual sardine landings recently analyzed by Jghab et al. (2019) in Morocco exhibit a marked inter-annual variability as well as a decreasing trend over the last four decades. Chl statistically explained the inter-annual variability of sardine catches, whereas a long-term weakening of the Atlantic inflow through the SoG, as inferred from tidal gauges (assuming geostrophic balance), was related to the negative trend of the series. Although to the best of our knowledge such weakening needs more solid observational evidence, the interpretation of a diminished AJ impacting negatively on sardine recruitment in southern AS *via* reduced advection of nutrients and spawning material from NW Alboran entails a potential interplay between fish populations in north and south Alboran, a topic that is currently being investigated (CopeMed II, 2017; CopeMed II, 2019). The crossing of the AS implies overcoming the physical barrier that the AJ represents. Although such a crossing is not the most likely pathway, evidence of cyclonic eddies trapping relatively cold and salty water (characteristic of north Alboran) off the African coast (Viúdez and Tintoré, 1995; García-Lafuente et al., 1998) suggests that north and south AS can be indeed connected through advection. The manner in which cyclonic eddies like the one shown in Figure 4 can travel from north to south across the AJ

is unknown. García-Lafuente et al. (1998, García-Lafuente et al., 2021) postulate that such eddies could have their origin in sharp meanders of the AJ pinched off near Cape Tres Forcas, where the AJ acquires maximum curvature. Similarly, the candidate location where meanders can separate from the main flow in eastern Alboran is the coastal region off Oran. Whatever the specific origin, these eddies represent intermittent north-to-south fluxes of nutrients, plankton, and fish early life stages whose role in the AS ecosystem and dynamics of fish populations is to be clarified.

7 Synthesis and future directions

The first conclusion that comes from this review is that important gaps in our understanding remain regarding what drives the variability of the basin-scale circulation of the AS, with alternance between double- and single-gyre types of circulation. These transitions have a seasonal signal, although abrupt transient events can take place year-round. Clues from observations and modeling point to the time dependence of the flow through the SoG (at atmospheric synoptic scale) as a likely driver for breaking down the most recurrent two-gyre system, although local wind stress and changes in the background stratification could also play a role (Peliz et al., 2013). A better understanding of the underlying cause (or causes) for these transitions would be needed to foresee potential changes in the AS circulation, perhaps favoring one flow type versus the other, related to climate change. The question has important biological consequences insofar as the different flow structures (one or two gyres) entail distinct pathways of the AJ, which brings nutrient-enriched water from the SoG, fertilizes the upper layer of the AS through its ageostrophic frontal dynamics, and is the primary source of meso- and submesoscale turbulence in the basin (Figure 4). Hence, the AJ has a major contribution to overall productivity (along with wind upwelling) and largely controls planktonic biomass distribution and dispersal of fish early life stages within the basin, ultimately shaping anchovy and sardine recruitment (and other's pelagic fish species) on both sides of the AS.



In a general context, the AS is within the Mediterranean, which is a recognized hotspot vulnerable to climate change (Giorgi, 2006). One likely near-future scenario for mid-latitude oceans such as the Mediterranean is the decline of primary productivity due to enhanced upper ocean stratification and reduced nutrient supply into the euphotic zone (Behrenfeld et al., 2006; Steinacher et al., 2010). In view of the variety of fertilization mechanisms reviewed here, some of which appear barely affected by climate change, such as the available mechanical tidal energy for diapycnal mixing in the SoG, the AS can be less prone to oligotrophization than other regions of the Mediterranean. Although speculative, this interpretation would be supported by the fact that SST in the AS has risen by $\sim 0.6^{\circ}\text{C}$ since 1997, similar to other areas of the Mediterranean, whereas surface Chl has not shown a clear trend (Figure 10). This contrasts with most of the Mediterranean regions, in which Chl is in decline. The null tendency of Chl also raises the question as to whether the primary environmental driver for the long-term decline of anchovy and sardine biomass and catches in the AS during the last decades, and perhaps that to be expected during the next decades, is the gradual loss of thermal habitat rather than food limitation.

Evaluations of future climate scenarios in the Mediterranean rely on ocean models operating at ~ 10 – 20 km horizontal resolution (Ruti et al., 2016; Macias et al., 2018; Soto-Navarro et al., 2020), resolving part of the mesoscale but missing its lower range and the submesoscale. The flow through the narrow SoG (14 km) is likewise poorly simulated in Mediterranean climate models. The short-scale processes impacting the circulation and primary productivity of the AS make it necessary to use dynamical downscaling solutions for (hopefully) more accurate evaluation and future projections of the regional sea climate. Another avenue for future work is the use of end-to-end (climate-to-fish) ecosystem models, which by

combining ocean circulation, lower trophic (nutrients, phytoplankton, and zooplankton), and fish submodels (Fiechter et al., 2021; Sánchez-Garrido et al., 2021), can help to better understand the dynamics of anchovy and sardine populations in response to climate variability and trends, offering new insights on how environmental perturbations (e.g., changes in circulation patterns, seawater temperature, etc.) are transmitted through the food web affecting early life stage survival, reproduction, bioenergetics, and ultimately recruitment.

Author contributions

JS-G conceived the original idea. IN reviewed the literature and processed the data and figures of the manuscript. JS-G wrote the bulk of the manuscript with inputs of IN. All authors listed have made a substantial, direct, and intellectual contribution to the work and approved it for publication.

Funding

The open access publication fees of this paper were partially covered by the University of Málaga.

Acknowledgments

IN acknowledges a predoctoral fellowship from the Spanish Ministry of Science and Innovation under the project BLUEMARO (PID2020-116136RB-100). This review has been conducted using E.U. Copernicus Marine Service Information. We thank Ana Giraldez and Manuel Hidalgo for providing the

historical catches series of anchovy and sardine shown in Figure 9.

Conflict of interest

The authors declare that the research was conducted in the absence of any commercial or financial relationships that could be construed as a potential conflict of interest.

References

- Agostini, V., and Bakun, A. (2002). 'Ocean triads' in the Mediterranean Sea: Physical mechanisms potentially structuring reproductive habitat suitability (With example application to European anchovy, *engraulis encrasicolus*). *Fish. Oceanogr.* 11 (3), 129–42. doi: 10.1046/j.1365-2419.2002.00201.x
- Alpert, W., Brandt, P., and Rubino, A. (2008). "Internal waves generated in the straits of Gibraltar and Messina: Observations from space," in *Remote sensing of the European seas*. Eds. V. Barale and M. Gade (Dordrecht: Springer). doi: 10.1007/978-1-4020-6772-3_24
- Armi, L. (1986). The hydraulics of two flowing layers with different densities. *J. Fluid. Mechanic.* 163, 27–58. doi: 10.1017/S0022112086002197
- Armi, L., and Farmer, D. M. (1988). The flow of Atlantic water through the strait of Gibraltar. *Prog. Oceanogr.* 21, 1–105. doi: 10.1016/0079-6611(88)90055-9
- Bakun, A. (1996). Patterns in the ocean. ocean processes and marine population dynamics (California, USA: University of California Sea Grant), 323 pp. in cooperation with Centro de Investigaciones Biológicas de Noroeste, La Paz, Baja California Sur, Mexico.
- Behrenfeld, M. J., O'Malley, R. T., Siegel, D. A., McClain, C., Sarmiento, J. L., Feldman, G. C., et al. (2006). Climate-driven trends in contemporary ocean productivity. *Nature* 444, 752–755. doi: 10.1038/nature05317
- Bormans, M., and Garrett, C. (1989). The effect of rotation on the surface inflow through the strait of Gibraltar. *Am. Meteorol. Soc.* 19 (10), 1535–1542. doi: 10.1175/1520-0485(1989)019<1535:TEOROT>2.0.CO;2
- Bray, N. A., Ochoa, J., and Kinder, T. H. (1995). The role of the interface in the exchange through the strait of Gibraltar. *J. Geophys. Res.* 100, 10755–10776. doi: 10.1029/95JC00381
- Brett, G. J., Pratt, L. J., Rypina, I. I., and Sánchez-Garrido, J. C. (2020). The Western alboran gyre: An analysis of its properties and its exchange with surrounding water. *J. Phys. Oceanogr.* 50 (12), 3379–3402. doi: 10.1175/JPO-D-20-0028.1
- Bryden, H. L., and Stommel, H. M. (1982). Origin of the Mediterranean outflow. *J. Mar. Res.* 40 (suppl.), 55–71.
- Candela, J., Winant, C. D., and Bryden, H. L. (1989). Meteorologically forced subinertial flows through the strait of Gibraltar. *J. Geophys. Res.* 94, 12667–12679. doi: 10.1029/JC094iC09p12667
- Capó, E., McWilliams, J. C., Mason, E., and Orfila, A. (2021). Intermittent frontogenesis in the Alboran Sea. *J. Phys. Oceanogr.* 51 (5), 1417–1439. doi: 10.1175/JPO-D-20-0277.1
- Cheney, R. E., and Doblar, R. A. (1982). Structure and variability of the Alboran Sea frontal system. *J. Geophys. Res.* 87, 585–594. doi: 10.1029/JC087iC01p00585
- CopeMed II (2017). *Report of the CopeMed II workshop on methodologies for the identification of stock units in the Alboran Sea* (Alicante, Spain), 58 pp. 3–6 April 2017. CopeMed II Technical documents N°46 (GCP/INT/028/SPA - GCP/INT/270/EC). Alicante.
- CopeMed II (2019). *Report of the mid-term workshop on TRANSBORAN project, "Transboundary population structure of sardine, European hake and blackspot seabream in the Alboran Sea and adjacent waters: A multidisciplinary approach"* (Malaga, Spain), 33 pp. 22–24 July 2019. CopeMed II Technical Documents N°52 (GCP/INT/028/SPA - GCP/INT/270/EC). Málaga.
- Davies, A. G., and Sleep, J. A. (1989). The photosynthetic response of nutrient-depleted dilute cultures of *skeltonema costatum* to pulses of ammonium and nitrate; the importance of phosphate. *J. Plankt. Res.* 11 (1), 141–164. doi: 10.1093/plankt/11.1.141
- Echevarría, F., García-Lafuente, J. G., Bruno, M., Gorsky, G., Goutx, M., Gonzalez, N., et al. (2002). Physical-biological coupling in the strait of Gibraltar. *Deep-Sea. Res. II.* 49 (19), 4115–4130. doi: 10.1016/S0967-0645(02)00145-5
- Eppley, R. W., Rogers, J. N., and McCarthy, J. J. (1969). Half-saturation constants for uptake of nitrate and ammonium by marine phytoplankton. *Limnol. Oceanogr.* 14, 912–920. doi: 10.4319/lo.1969.14.6.0912
- Esposito, G., Berta, M., Centurioni, L., Johnston, T. M. S., Lodise, J., Özgökmen, T., et al. (2021). Submesoscale vorticity and divergence in the Alboran Sea: Scale and depth dependence. *Front. Mar. Sci.* 8. doi: 10.3389/fmars.2021.678304
- Fiechter, J., Pozo Buil, M., Jacox, M. G., Alexander, M. A., and Rose, K. A. (2021). Projected shifts in 21st century sardine distribution and catch in the California current. *Front. Mar. Sci.* 8. doi: 10.3389/fmars.2021.685241
- Flexas, M. M., Gomis, D., Ruiz, S., Pascual, A., and Leon, P. (2006). *In situ* and satellite observations of the Eastward migration of the Western Alboran Sea gyre. *Prog. Oceanogr.* 70, 486–509. doi: 10.1016/j.pcean.2006.03.017
- García, A. (2006). Estudio sobre la variabilidad del crecimiento larvario de la sardina (*Sardina pilchardus*, walbaum) del mar de alborán (Spain: University of Vigo).
- García-Jove, M., Mourre, B., Zarokanellos, N. D., Lermusiaux, P. F. J., Rudnick, D. L., and Tintoré, J. (2022). Frontal dynamics in the Alboran Sea: 2. processes for vertical velocities development. *J. Geophys. Res.: Ocean.* 127, e2021JC017428. doi: 10.1029/2021JC017428
- García-Lafuente, J., Cano, N., Vargas, M., Rubin, J. P., and Guerra, A. (1998). Evolution of the Alboran Sea hydrographic structures during July 1993. *Deep-Sea. Res.* 45, 39–65. doi: 10.1016/S0967-0637(97)00216-1
- García-Lafuente, J., Vargas, J. M., Plaza, F., Sarhan, T., Candela, J., and Bascheck, B. (2000). Tide at the Eastern section of the strait of Gibraltar. *J. Geophys. Res.: Ocean.* 105 (C6), 14197–14213. doi: 10.1029/2000JC900007
- García-Lafuente, J., Alvarez, E., Vargas, J. M., and Ratsimandresy, W. (2002). Subinertial variability in the flow through the strait of Gibraltar. *J. Geophys. Res.* 107 (C10), 32.1–32.9. doi: 10.1029/2001JC0011004
- García-Lafuente, J., and Delgado, J. (2004). The meandering path of a drifter around the Western alboran gyre. *J. Phys. Oceanogr.* 34 (3), 685–692. doi: 10.1175/3516.1
- García-Lafuente, J., Bruque Pozas, E., Sánchez-Garrido, J. C., Sannino, G., and Sammartino, S. (2013). The interface mixing layer and the tidal dynamics at the Eastern part of the strait of Gibraltar. *J. Mar. Syst.*, 117–118. doi: 10.1016/j.jmarsys.2013.02.014
- García-Lafuente, J., Sánchez-Garrido, J. C., García, A., Hidalgo, M., Sammartino, S., Laiz, R., et al. (2021). Biophysical processes determining the connectivity of the Alboran Sea fish populations. In J. C. Báez, J. T. Vázquez, J. A. Caminas and M. Malouli (editors) *Alboran Sea – Ecosystems and marine resources*. Springer Nature Switzerland AG.
- García, A., Laiz-Carrión, R., Cortés, D., Quintanilla, J., Uriarte, A., Ramírez, T., et al. (2021). "Chapter 13: Evolving from fry fisheries to early life research on pelagic fish resources," in *Alboran Sea – ecosystems and marine resources*. Eds. J. C. Báez, J. T. Vázquez, J. A. Caminas and M. Malouli (Cham, Switzerland: Springer Nature Switzerland AG), ISBN: .
- Garrett, C., Bormans, M., and Thomson, K. R. (1990). "Is the exchange through the strait of Gibraltar maximal or submaximal?," in *The physical oceanography of Sea straits*, vol. 318. Ed. L. J. Pratt (Dordrecht: Springer), 271–294. (Mathematical and Physical Sciences). doi: 10.1007/978-94-009-0677-8_13
- Giorgi, F. (2006). Climate change hot-spots. *Geophys. Res. Lett.* 33, 1–4. doi: 10.1029/2006GL025734
- Giráldez, A. (2021). "Chapter 16: Small pelagic resources: A historic perspective and current state of the resources," in *Alboran Sea – ecosystems and marine resources*. Eds. J. C. Báez, J. T. Vázquez, J. A. Caminas and M. Malouli (Cham, Switzerland: Springer Nature Switzerland AG), ISBN: .

Publisher's note

All claims expressed in this article are solely those of the authors and do not necessarily represent those of their affiliated organizations, or those of the publisher, the editors and the reviewers. Any product that may be evaluated in this article, or claim that may be made by its manufacturer, is not guaranteed or endorsed by the publisher.

- Gómez, F., Echevarría, F., García, C. M., Prieto, L., Ruiz, L., Reul, A., et al. (2000). Microplankton distribution in the strait of Gibraltar: Coupling between organisms and hydrodynamics structures. *J. Plankt. Res.* 22, 603–617. doi: 10.1093/plankt/22.4.603
- Gomis, D., Ruiz, S., and Pedder, M. A. (2001). Diagnostic analysis of the 3D ageostrophic circulation from a multivariate spatial interpolation of CTD and ADCP data. *Deep-Sea. Res. Part I: Oceanogr. Res. Paper.* 48 (1), 269–295. doi: 10.1016/S0967-0637(00)00060-1
- Hersbach, H., Bell, B., Berrisford, P., Biavati, G., Horányi, A., Muñoz Sabater, J., et al. (2018). *The ERA5 global reanalysis.* *Q J R Meteorol. Soc.* 146, 1994–2049. doi: 10.24381/cds.adbb2d47
- Holton, J. R. (2004). *Introduction to dynamic meteorology. 4th Edition* (Amsterdam: Elsevier), 535.
- Huertas, I. E., Ríos, A. F., García-Lafuente, J., Navarro, G., Makaoui, A., Sánchez-Roman, A., et al. (2012). Atlantic Forcing of the Mediterranean oligotrophy. *Global Biogeochem. Cy.* 26, GB2022. doi: 10.1029/2011GB004167
- Jackson, C. R., and Apel, J. (2004). *An atlas of internal solitary-like waves and their properties. 2nd ed* (Alexandria, Va: Global Ocean Assoc.). Available at: <http://www.internalwaveatlas.com/>.
- Jghab, A., Vargas-Yañez, M., Reul, A., García-Martínez, M. C., Hidalgo, M., Moya, F., et al. (2019). The influence of environmental factors and hydrodynamics on sardine (*Sardina pilchardus*, walbaum 1792) abundance in the southern Alboran Sea. *J. Mar. Syst.* 191, 51–63. doi: 10.1016/j.jmarsys.2018.12.002
- Kinder, T. H., and Bryden, H. L. (1990). “Aspiration of deep waters through straits,” in *The physical oceanography of Sea straits*. Ed. L. J. Pratt (Dordrecht, The Netherlands: Kluwer Academic Publishers), 295–319, ISBN: .
- La Violette, P. E. (1984). The advection of cyclonic submesoscale thermal features in the Alboran Sea. *Journal of Physical Oceanography* 14 (3), 550–565. doi: 10.1175/1520-0485(1984)014<0550:TAOSTF>2.0.CO;2.
- La Violette, P., and Lacombe, H. (1988). Tidal-induced pulses in the flow through the Strait of Gibraltar. *Oceanol. Acta* 13–27.
- Macías, D., Navarro, G., Bartual, A., Echevarría, F., and Huertas, I. E. (2009). Primary production in the strait of Gibraltar: Carbon fixation rates in relation to hydrodynamic and phytoplankton dynamics. *Estuar. Coast. Shelf. Sci.* 83, 197–210. doi: 10.1016/j.ecss.2009.03.032
- Macías, D., Stips, A., García-Gorriç, E., and Dosio, A. (2018). Hydrological and biogeochemical response of the Mediterranean Sea to freshwater flow changes for the end of the 21st century. *PLoS ONE* 13, e0192174. doi: 10.1371/journal.pone.0192174
- Manca, B., Burca, M., Giorgetti, A., Coatanoan, C., Garcia, M. J., and Iona, A. (2004). Physical and biochemical averaged vertical profiles in the Mediterranean regions: An important tool to trace the climatology of water masses and to validate incoming data from operational oceanography. *J. Mar. Syst.* 48, 83–116. doi: 10.1016/j.jmarsys.2003.11.025
- McWilliams, J. C. (2021). Oceanic frontogenesis. *Annu. Rev. Mar. Sci.* 13, 227–253. doi: 10.1146/annurev-marine-032320-120725
- McWilliams, J. C., Gula, J., and Molemaker, M. J. (2019). The gulf stream north wall: Ageostrophic circulation and frontogenesis. *J. Phys. Oceanogr.* 49 (4), 893–916. doi: 10.1175/JPO-D-18-0203.1
- Moran, X. A. G., and Estrada, M. (2001). Short-term variability of photosynthetic parameters and particulate and dissolved primary production in the Alboran Sea (SW Mediterranean). *Mar. Ecol. Prog. Ser.* 212, 53–67. doi: 10.3354/meps212053
- Naranjo, C., García-Lafuente, J., Sannino, G., and Sánchez-Garrido, J. C. (2014). How much do tides affect the circulation of the Mediterranean Sea? from local processes in the strait of Gibraltar to basin-scale effects. *Progress in Oceanography*. 127, 108–116. doi: 10.1016/j.pocean.2014.06.005
- Naranjo, C., Sannino, G., García-Lafuente, J., Bellanco, M., and Taupier-Letage, I. (2015). Mediterranean Waters along and across the strait of Gibraltar, characterization and zonal modification. *Deep-Sea. Res. I.* 105, 41–52. doi: 10.1016/j.dsr.2015.08.003
- Navarro, G., Vázquez, A., Macías, D., Bruno, M., and Ruiz, J. (2011). Understanding the patterns of biological response to physical forcing in the Alboran Sea (Western Mediterranean). *Geophys. Res. Lett.* 38, L23606. doi: 10.1029/2011GL049708
- Newton, C. W. (1978). Fronts and wave distributions in gulf stream and atmospheric jet stream. *J. Geophys. Res.* 83 (9), 4697–4706. doi: 10.1029/JC083iC09p04697
- Oguz, T., Macías, D., García-Lafuente, J., Pascual, J., and Tintoré, J. (2014). Fueling plankton production by a meandering frontal jet: A case study for the Alboran Sea (Western Mediterranean). *PLoS One* 9 (11), e111482. doi: 10.1371/journal.pone.0111482
- Parrilla, G., and Kinder, T. H. (1984). The Physical Oceanography of the Alboran Sea, [Rep] 40 (1), 143–184. Oceanogr. Group Div. of Applied Sciences, Harvard Univ.
- Pascual, A., Ruiz, S., Olita, A., Troupin, C., Claret, M., Casas, B., et al. (2017). A multiplatform experiment to unravel meso- and submesoscale processes in an intense front (AlborEx). *Front. Mar. Sci.* 4. doi: 10.3389/fmars.2017.00039
- Peliz, A., Boutov, D., and Teles-Machado, A. (2013). The Alboran Sea mesoscale in a long-term resolution simulation: Statistical analysis. *Ocean. Model.* 72, 32–52. doi: 10.1016/j.ocemod.2013.07.002
- Perkins, H., Kinder, T., and La-Violette, P. (1990). The Atlantic inflow in the Western Alboran Sea. *J. Phys. Oceanogr.* 20, 242–263. doi: 10.1175/1520-0485(1990)020<0242:TAITW>2.0.CO;2
- Pratt, L. J., and Whitehead, J. A. (2008). *Rotating hydraulics: Nonlinear topographic effects in the ocean and atmosphere* Vol. 36 (New York, NY: Springer), 589 pp. Atmos. Ocean. Sci. Libr.
- Ramírez, E., Macías, D., García, C. M., and Bruno, M. (2014). Biogeochemical patterns in the Atlantic inflow through the strait. *Deep. Sea. Res.* 85, 88–100. doi: 10.1016/j.dsr.2013.12.004
- Ramírez, T., Muñoz, M., Reul, A., García-Martínez, C., Moya, F., Vargas-Yañez, M., et al. (2021). “Chapter 7: The biogeochemical context of marine planktonic ecosystems,” in *Alboran Sea – ecosystems and marine resources*. Eds. J. C. Báez, J. T. Vázquez, J. A. Caminas and M. Malouli (Springer Nature Switzerland AG), ISBN: .
- Renault, L., Oguz, T., Pascual, A., Vizoso, G., and Tintore, J. (2012). Surface circulation in the alborn Sea (Western Mediterranean) inferred from remotely sensed data. *J. Geophys. Res.* 117 (8), 1–11. doi: 10.1029/2011JC007659
- Ruiz, S., Claret, M., Pascual, A., Olita, A., Troupin, C., Capet, A., et al. (2019). Effects of oceanic mesoscale and submesoscale frontal processes on the vertical transport of phytoplankton. *J. Geophys. Res.: Ocean.* 124 (8), 5999–6014. doi: 10.1029/2019JC015034
- Ruiz, J., Macías, D., Rincón, M., Pascual, A., Catalán, I. A., and Navarro, G. (2013). Recruiting at the edge: Kinetic energy inhibits anchovy populations in the Western Mediterranean. *PLoS One* 8 (2), e55523. doi: 10.1371/journal.pone.0055523
- Ruti, P. M., Somot, S., Giorgi, F., Dubois, C., Flaounas, E., Obermann, A., et al. (2016). Med-CORDEX initiative for Mediterranean climate studies. *Bull. Am. Meteorol. Soc.* 97 (7), 1187–1208. doi: 10.1175/BAMS-D-14-00176.1
- Sánchez-Garrido, J. C., Fiechter, J., Rose, K. A., Werner, F. E., and Curchitser, E. N. (2021). Dynamics of anchovy and sardine populations in the canary current off NW Africa: Responses to environmental and climate forcing in a climate-to-Fish ecosystem model. *Fish. Oceanogr.* 30, 232–2252. doi: 10.1111/fog.12516
- Sánchez-Garrido, J. C., García-Lafuente, J., Álvarez Fanjul, E., García Sotillo, M., and de los Santos, F. J. (2013). What does cause the collapse of the Western alboran gyre? results of an operational ocean model. *Prog. Oceanogr.* 116, 142–153. doi: 10.1016/j.pocean.2013.07.002
- Sánchez-Garrido, J. C., García-Lafuente, J., Criado Aldeanueva, F., Baquerizo, A., and Sannino, G. (2008). Time-spatial variability observed in velocity of propagation of the internal bore in the strait of Gibraltar. *J. Geophys. Res.* 113, C07034. doi: 10.1029/2007JC004624
- Sánchez Garrido, J. C., Naranjo, C., Macías, D., García-Lafuente, J., and Oguz, T. (2015). Modeling the impact of tidal flows on the biological productivity of the Alboran Sea. *J. Geophys. Res.: Ocean.* 120 (11), 7329–7345. doi: 10.1002/2015JC010885
- Sánchez-Garrido, J. C., Sannino, G., Liberti, L., García-Lafuente, J., and Pratt, L. (2011). Numerical modeling of three-dimensional stratified tidal flow over camarinal sill, strait of Gibraltar. *J. Geophys. Res.* 116, C12026. doi: 10.1029/2011JC007093
- Sannino, G., Pratt, L., and Carillo, A. (2009). Hydraulic criticality of the exchange flow through the strait of Gibraltar. *J. Phys. Oceanogr.* 39, 2779–2799. doi: 10.1175/2009JPO4075.1
- Sarhan, T., García-Lafuente, J., Vargas, M., Vargas, J. M., and Plaza, F. (2000). Upwelling mechanisms in the northwestern Alboran Sea. *J. Mar. Syst.* 23 (4), 317–331. doi: 10.1016/S0924-7963(99)00068-8
- Soto-Navarro, J., Criado-Aldeanueva, F., García-Lafuente, J., and Sánchez-Román, A. (2010). Estimation of the Atlantic inflow through the strait of Gibraltar from climatological and *in situ* data. *J. Geophys. Res.* 115, C10023. doi: 10.1029/2010JC006302
- Soto-Navarro, J., Jordá, G., Amores, A., Cabos, W., Somot, S., Sevault, F., et al. (2020). Evolution of Mediterranean Sea water properties under climate change scenarios in the med-CORDEX ensemble. *Climate Dyn* 54, 2135–2165. doi: 10.1007/s00382-019-05105-4
- Spall, M. A. (1995). Frontogenesis, subduction, and cross-front exchange at upper ocean fronts. *J. Geophys. Res.* 100 (C2), 2543–2557. doi: 10.1029/94JC02860

- Steinacher, M., Joos, F., Frölicher, T., Bopp, L., Cadule, P., Cocco, V., et al. (2010). Projected 21st century decrease in marine productivity: A multi-model analysis. *Biogeosciences* 7, 979–1005. doi: 10.5194/bg-7-979-2010
- Tintoré, J., Wang, D., and La Violette, P. E. (1990). Eddies and thermohaline intrusions of the Shelf/Slope front off the northeast Spanish coast. *J. Geophys. Res.* 95. doi: 10.1029/JC095iC02p01627. issn: 0148-0227.
- Troupin, C., Pascual, A., Ruiz, S., Olita, A., Casas, B., Margirier, F., et al. (2019). The AlborEX dataset: Sampling of Sub-mesoscale features in the Alboran Sea. *Earth Syst. Sci. Data* 11, 129–145. doi: 10.5194/essd-11-129-2019
- Uitz, J., Stramski, D., Gentili, B., D'Ortenzio, F., and Claustre, H. (2012). Estimates of phytoplankton class-specific and total primary production in the Mediterranean Sea from satellite ocean color observations. *Global Biogeochem. Cycle* 26 (2). doi: 10.1029/2011GB004055
- Vargas-Yáñez, M., García-Martínez, M., Moya, F., Balbín, R., and López-Jurado, J. (2021). "Chapter 4: The oceanographic and climatic context," in *Alboran Sea – ecosystems and marine resources*. Eds. J. C. Báez, J. T. Vázquez, J. A. Caminas and M. Malouli (Springer Nature Switzerland AG), ISBN: . doi: 10.1007/978-3-030-65516-7_4
- Vargas-Yáñez, M., Giráldez, A., Torres, P., González, M., García-Martínez, M.C., Moya, F., et al (2020). "Variability of oceanographic and meteorological conditions in the northern Alboran Sea at seasonal, interannual and long-term time scales and their influence on sardine (*Sardina pilchardus*, Walbaum 1792) landings. *Fish. Oceanogr.* 1–14. doi: 10.1111/fog.12477
- Vargas-Yáñez, M., Plaza, F., García-Lafuente, J., Sarhan, T., Vargas, J. M., and Vélez-Belchi, P. (2002). About the seasonal variability of the Alboran Sea circulation. *J. Mar. Syst.* 35 (3–4), 229–248. doi: 10.1016/S0924-7963(02)00128-8
- Vélez-Belchi, P., Vargas-Yáñez, M., and Tintoré, J. (2005). Observation of a Western alboran gyre migration. *Progr. Oceanogr.* 66, 190–210. doi: 10.1016/j.pocean.2004.09.006
- Viúdez, A., and Haney, R. L. (1997). On the relative vorticity of the Atlantic jet in the Alboran Sea. *J. Phys. Oceanogr.* 27, 175–185. doi: 10.1175/1520-0485(1997)027<0175:OTRVOT>2.0.CO;2
- Viúdez, A., and Tintoré, J. (1995). Time and space variability in the Eastern Alboran Sea from march to may 1990. *J. Geophys. Res.* 100 (C5), 8571–8586. doi: 10.1029/94JC03129
- Vlasenko, V., Brandt, P., and Rubino, A. (2000). Structure of Large-amplitude internal solitary waves. *J. Phys. Oceanogr.* 30 (9), 2172–2185. doi: 10.1175/1520-0485(2000)030<2172:SOLAIS>2.0.CO;2
- Vlasenko, V., Sánchez Garrido, J. C., Stashchuk, N., García-Lafuente, J., and Losada, M. (2009). Three-dimensional evolution of Large-amplitude internal waves in the strait of Gibraltar. *J. Phys. Oceanogr.* 39, 2230–2246. doi: 10.1175/2009JPO4007.1
- Wesson, J. C., and Gregg, M. C. (1994). Mixing at camarinall sill in the strait of Gibraltar. *J. Geophys. Res. Ocean.* 99, 9847–9878. doi: 10.1029/94JC00256
- Whitehead, J. A., and Miller, A. R. (1979). Laboratory simulation of the gyre in the Alboran Sea. *J. Geophys. Res.* 84. doi: 10.1029/JC084iC07p03733. issn: 0148-0227.
- Williams, R. G., and Follows, M. J. (2003). Physical transport of nutrients and the maintenance of biological production. *Ocean. Biogeochem., The Role of the Ocean Carbon Cycle in Global Change* M.J.R Fasham (Springer Nature Switzerland).
- Zarokanellos, N. D., Rudnick, D. L., Garcia-Jove, M., Mourre, B., Ruiz, S., Pascual, A., et al. (2022). Frontal dynamics in the Alboran Sea: 1. coherent 3D pathways at the almeria-Oran front using underwater glider observations. *J. Geophys. Res.: Ocean.* 127, e2021JC017405. doi: 10.1029/2021JC017405